Al-Maisari, Abdullah; Ma, Zhongcheng; Havula, Jarmo; Lu, Wei; Puttonen, Jari

Method For Determining the Cross-Sectional Resistance of Transversely Corrugated Cold-Formed Steel Arches Under Compression

Published in:
ce/papers

DOI:
10.1002/cepa.2477

Published: 01/09/2023

Document Version
Publisher's PDF, also known as Version of record

ce/papers Proceedings in civil engineering

Ernst & Sohn A Wiley Brand

ORIGINAL ARTICLE

eurosteel AMSTERDAM 2023

Ernst & Sohn A Wiley Brand

Method For Determining the Cross-Sectional Resistance of Transversely Corrugated Cold-Formed Steel Arches Under Compression

Abdullah Al-Maisari[1,2] | Zhongcheng Ma[1] | Jarmo Havula[1] | Wei Lu[2] | Jari Puttonen[2]

Correspondence

Dr. Zhongcheng Ma
Häme University of Applied Sciences
HAMK Tech Research Unit
Vankanlähde 13
13100 Hämeenlinna, Finland
Email: zma@hamk.fi

[1] HAMK Tech Research Unit, Häme University of Applied Sciences, Hämeenlinna, Finland
[2] Department of Civil Engineering, Aalto University, Espoo, Finland

Abstract

Transversely corrugated cold-formed steel (CFS) arch elements are widely used as self-supporting building roofs. The transverse corrugations and the unusual cross-section shapes complicate the design of such members under compressive loading. Since the current Eurocode does not cover the design rules for CFS arches with transverse corrugations, the objective of this study is to develop a method for determining the effective cross-section of such members under compression load. In total 36 stiffness tests and 27 compression tests were carried out on the corrugated CFS arches with different thicknesses and curvatures. Steel arch profiles with thickness of 1.5 mm has 55% higher ultimate load value than the profiles with 1.1 mm thickness due to a bigger effective area to resist the axial compressive forces. The smaller the steel arch radius is, the more susceptible it is to buckle and stability failure due to the eccentricity of compression load along the curvature. The stiffness is directly proportional to the thickness and inversely proportional to the radius of the steel arches. Based on the thickness and the radius, the correction factors between 0.90 and 1.37 are proposed for determining the resistance of curved steel arches with corrugations. The method developed in this research can be used for designing similar types of arches.

Keywords

Cold-formed steel, steel arches, transverse corrugations, ultimate compression strength, stiffness tests

1 Introduction

Cold-formed steel arches are common structural elements used in buildings. The arches are created by bending corrugated steel sheets into a desired shape and are then joined together by press bending. The use of cold-formed steel arches creates structures that are both light and strong and suitable for a variety of uses. The example applications are warehouses and farm buildings. This design is cost-effective because the arches work as load-bearing elements and a part of the envelope at the same time. In addition, other benefits of these steel arches include versatility in shaping, simplicity in production, and simplicity in installation. Buildings made of arch panels can span up to 40 meters and resist extreme weather. [1,2]

The structures using cold-formed steel components in Europe are designed according to EN 1993-1-3 [3] and EN 1993-1-5 [4]. However, these design standards do not include the rules for designing compressive strength of curved elements. The design of such members under compressive loads is further complicated by the existence of the transverse corrugations, which both stiffen and bend the thin-walled steel sheet into a curved shape. To determine the strengths of such panels with built-in transverse stiffeners, experimental tests are necessary. Numerous articles [5-8] about corrugated curved steel arches have discussed several experimental and numerical approaches to study the behaviour of such members. In this paper, the tests were carried out to investigate the effects of steel arch curvature and transverse corrugations on the compressive behaviour of steel arch profiles.

2 Effective cross-section of steel arch profile

For practical design, the cross section of the steel arch profile has been often idealized as the section shown in Figure 1. The profile is often assumed to be flat so that EN 1993-1-3 and EN 1993-1-5 can be used to calculate the effective plate widths of webs, lower flange, upper flanges, double edge stiffener and triple edge stiffener.

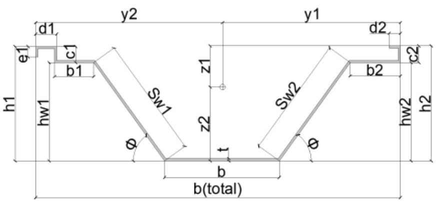

Figure 1 Theoretical/Idealized cross section

https://doi.org/10.1002/cepa.2477

For plane elements without stiffeners, the effective widths of unstiffened elements should be obtained from EN 1993-1-5 using the notional flat width by determining the reduction factors for plate buckling based on the plate slenderness λ. The reduction factor ρ is taken as follows:

Internal compression elements:

$$\rho = 1.0 \qquad \forall \ \lambda \leq 0.673 \tag{1.1}$$

$$\rho = \frac{\lambda - 0.055*(3+\Psi)}{\lambda^2} < 1 \qquad \forall \ \lambda > 0.673 \tag{1.2}$$

– Outstand compression elements:

$$\rho = 1.0 \qquad \forall \ \lambda \leq 0.748 \tag{1.3}$$

$$\rho = \frac{\lambda - 0.188}{\lambda^2} < 1 \qquad \forall \ \lambda > 0.748 \tag{1.4}$$

The plate slenderness λ_p is given by:

$$\lambda = \frac{b}{t*28.4*\varepsilon\sqrt{k_\sigma}} \tag{2}$$

$$\varepsilon = \sqrt{235/f_y} \tag{3}$$

where b and t are the width and the thickness of the plate element, respectively; k_σ is the buckling coefficient; and f_y is the yield strength of the steel; Ψ is the stress ratio.

The distortional buckling of the cross-section with edge stiffeners is considered by reducing the thickness of the edge stiffeners. The elastic critical buckling stress $\sigma_{cr,s}$ for an edge stiffener is obtained from:

$$\sigma_{cr,s} = \frac{2*\sqrt{K*E*I_s}}{A_s} \tag{4}$$

where I_s is the effective second moment of area for stiffeners, taken as that of its area A_s about the centroid axis of effective cross section. K is the spring stiffness (k) per unit length of specimen (l). Since the design code only provide the spring stiffness of C and Z shape profile, the spring stiffness (k) of the profile of the curved steel arch with corrugations need to be determined by horizontal and vertical stiffness tests. Once the stiffness factor is determined, the relative slenderness can be calculated using the equation (6) with the equation (4). The reduction factor χ_d for the distortional buckling resistance (flexural buckling of a stiffener) is obtained from the equations (5) based on the value of the relative slenderness λ_d.

$$\chi_d = 1 \qquad \Rightarrow \lambda_d \leq 0.65 \tag{5.1}$$

$$\chi_d = 1.47 - 0.723 * \lambda_d \qquad \Rightarrow 0.65 < \lambda_d < 1.38 \tag{5.2}$$

$$\chi_d = \frac{0.66}{\lambda_d} \qquad \Rightarrow \lambda_d \geq 1.38 \tag{5.3}$$

$$\lambda_d = \sqrt{f_{yb}/\sigma_{cr,s}} \tag{6}$$

The thickness reduction (χ_d) for the edge stiffeners is applied and is used later in the calculation of the effective area of cross section.

The Eurocode 1993-1-3 does not cover the design of cold-formed members with corrugations. Additionally, the triple edge folds are not covered by the Eurocode 1993-1-3, hence the experimental testing and FEM analysis are the only options to determine the properties of effective cross section. Edge stiffeners are supposed to improve the distortional buckling resistance by distributing applied forces more evenly across the section. Due to the geometry of the triple edge stiffener, vertical and horizontal stiffness tests were conducted.

Figure 2 shows the effective widths of plate elements for the idealized cross section of steel arch. The cross-sectional resistance under compression loads is determined by multiplying the effective cross-section area with the yield strength of steel. As the idealized flat section does not include the effects of transverse corrugations, correction factors are needed for predicting the actual resistance of arches.

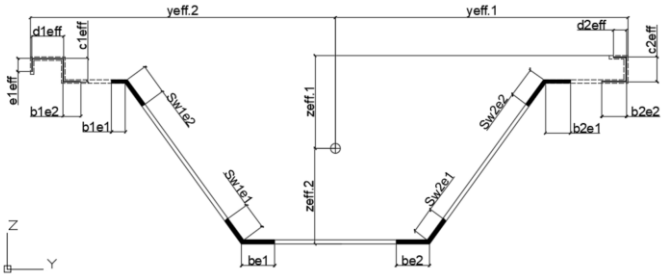

Figure 2 Effective cross section under uniaxial compression

3 Experimental tests

Two types of tests were conducted: uniaxial compression and stiffness tests. The compression tests are for obtaining the cross-sectional resistance and the stiffness tests are for obtaining the stiffness of edge stiffeners to determine their reduced thickness. Additionally, the coupon tests were carried out to determine the effect of plate thickness and cold forming on the yield strength of these types of steel arch elements.

3.1 Compression test

A total number of 27 tests were conducted to study the effects of thickness and curvature on the behaviour of the arches under compression. Three thicknesses were investigated, i.e., 1.1 mm, 1.2 mm, and 1.5 mm with three radii of the steel arches: 6 m, 12 m, and 24 m.

3.1.1 Preparation of the test specimens

Specimens are cut to a length of 750 mm. For more reliable result, it is essential to distribute the load uniformly over the whole cross- sectional area of the steel arch elements. Hence the concrete blocks were casted on both ends of the steel arch elements. Before preparing the concrete blocks, it was checked that the strength of concrete was large enough to withstand the pressure generated by the cross-section of samples during the test.

The specimen was then inserted into the concrete mould on the top of the spacers as shown in figure 3 (b). The edges of the steel arch profiles were thin and sharp, which could create large pressure in the concrete during the test resulting in shear failure. As a solution, 9 screws (118 mm long SDT14-5.5) were drilled through the edges of the test specimens. The screws helped prevent the cut off failure between the concrete and the specimens. The reinforcement bars were used for strengthening the concrete especially for testing stronger specimens so that the concrete blocks did not collapse.

Before pouring the concrete, the specimens were ensured to be as vertical as possible. The specimen embedment length with the concrete was about 50 mm on both sides. The span length was chosen to be 650 mm in reference to Annex A.3.2 clause (2) in SFS EN 1993-1-3. The clause states that the specimen should have a length of at least 3 times the width of the widest plate element. The webs were the widest plates of the steel arch cross section (216 mm). Upon the completion of concrete casting at both ends of the specimen, the concrete blocks were left to cure for at least a period of 28 day to ensure full strength.

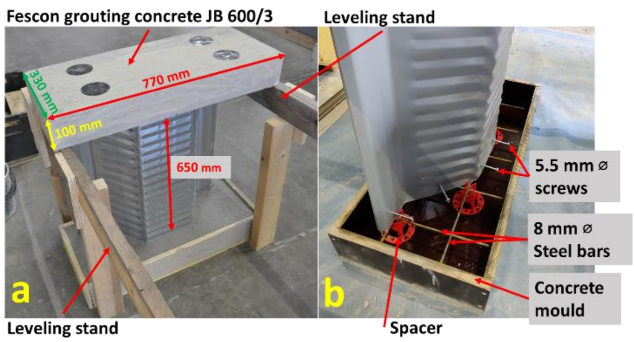

Figure 3 Sample preparation (a) after concreting (b) before concreting

3.1.2 Loading location based on the centroid of the cross-section

The effective centroid in the critical axis (z-direction) of the cross-section with the corrugations was calculated. Besides, steel arch specimens were simulated using FEM software to determine the loading point in order to ensure the uniform compression in the cross section. Based on the simulation results, the best loading position was determined as a distance of 150 mm from the bottom surface of the specimen and 330 mm from the edge of the double edge stiffener as shown in figure 4.

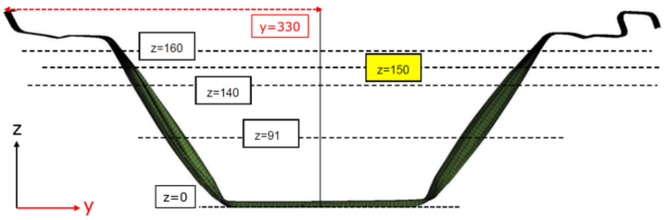

Figure 4 Different loading applying positions tested during simulation

3.1.3 Test setup

Figure 5 shows the setup for the compression test. The load was applied to the pre-determined location through a hydraulic load cell. A rectangular steel profile was placed in between load cell and test sample to distribute the load over the effective centroid of the cross section more evenly. To avoid excessive shift of the effective centroid of the specimen under uniaxial compression, the initial loading position of compressive force was exactly at the effective centroid (y,z) calculated for the cross section of steel arch profiles. To prevent any unwanted twisting of the sample during the test, two steel rods were used to clamp the upper concrete block of the sample.

Displacement sensors were used to measure the deformation of the samples during the test. In Figure 5, the displacement sensor [D1] is the one connected to the load cell. Displacement sensor [D2] is placed along the double edge stiffener. Displacement sensor [D3] is located near the triple edge stiffener. Finally, Displacement sensor [D4] is mounted to middle of the corrugated flange as shown in figure 5. The gauge distance for displacement sensors D2-D4 is 500 mm.

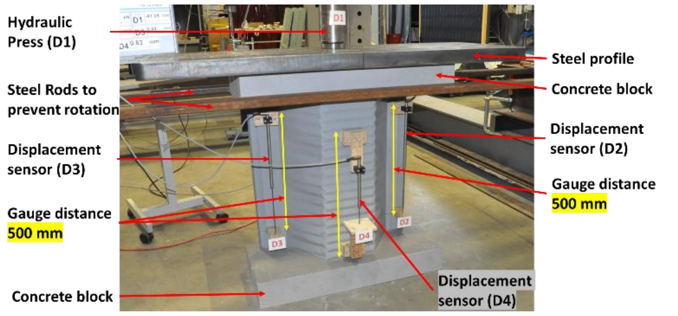

Figure 5 Test arrangement for compression test

The loading was applied to the specimen as a constant movement of the hydraulic cylinder with a speed of 1.5 mm/min. The tests were stopped when the load has dropped to less than 40% of the ultimate load. The data from the load cell and displacement sensors were then recorded to produce the load-displacement curves.

3.2 Stiffness test

Due to the shape of the cross section with corrugation and stiffeners, the stiffness tests were conducted to measure vertical and horizontal stiffness, respectively. The spring stiffness K in Eq. 4 was determined by these tests for the edge stiffeners. In total 36 specimens were used for both stiffness tests.

3.2.1 Setup for defining horizontal stiffness

Figure 6 shows the general testing arrangement for horizontal stiffness test. The span length of profiles was 600 mm. A steel plate was attached to the arch element to uniformly distribute the load throughout the profile while performing the test. The horizontal force was applied by using the threaded bar, which was fastened to generate the bending force in the webs.

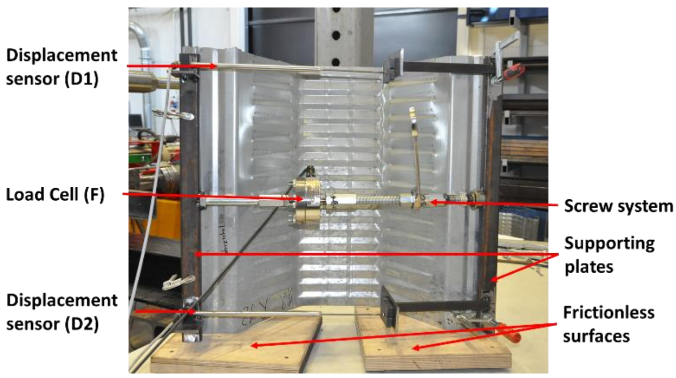

Figure 6 Test arrangement for horizontal stiffness test

Four full cycles were performed to ensure consistency and validity of the force displacement curve. A 50 kN load cell was used to measure the force generated during the test. Two displacement sensors were used to measure the horizontal displacement between the webs. The profile was then placed over frictionless surface to avoid any external force created by friction during the test.

3.2.2 Setup for defining vertical stiffness

Figure 7 shows the arrangement for defining vertical stiffness. In this test, a vertical force is applied on the weaker side (Side A). Similarly, the span length of tested profiles was 600 mm on average. In total 5 loading cycles were performed in each test. The vertical spring stiffness value defined based on the last cycle.

A 50 kN hydraulic pressing cylinder was used to measure the force generated by forced displacements during the test. The phases of one complete loading cycle sequence were: (0 mm → (-20 mm) → 0 mm → (+20 mm) →0 mm).

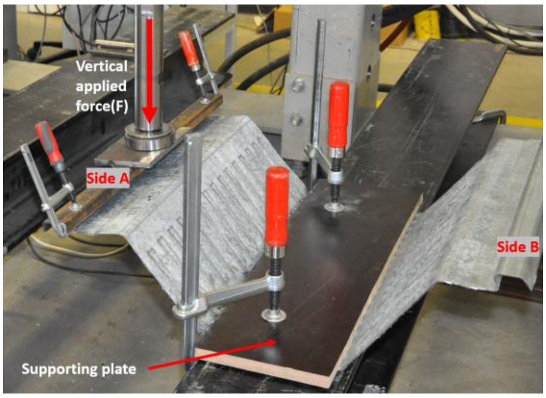

Figure 7 Test arrangement for vertical stiffness test

4 Results and discussion

4.1 Compression test results

Figure 8 shows the deformations and buckling modes of some specimens received in compression tests, where a typical failure for most samples was local buckling which led to wrinkling in the region consisting of the corrugated upper flange-web joint, upper flange and double edge stiffener (the cycled area in Figure 8). Most deformation happened at the weak side of double edge stiffener. The observed local buckling failure modes confirmed the necessity to determine the effective area of the cross-sections.

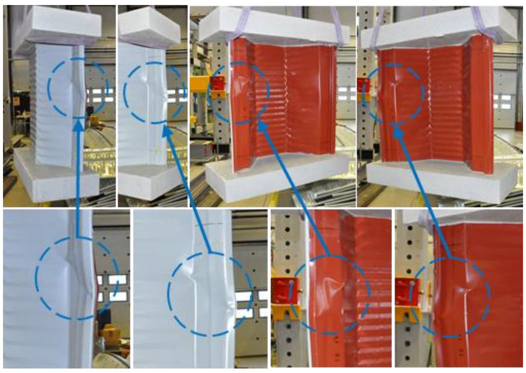

Figure 8 Typical failure modes of compression tests

During the compression test, the concrete integrity was intact, and no major failure happened in either of the concrete blocks. The displacement sensors were attached to the steel arch body instead of the concrete blocks in order to eliminate any deformations that might happen due to the interaction of steel arch profile and concrete body.

Figure 9 shows the force and displacement diagram measured by the load cell transducer D1 for the 1.5 mm thick profile with radii of 6 m, 12 m, and 24 m, respectively. The results also show that the ultimate load carrying capacity depends on the radius of the arch. The smaller the radius of steel arch profiles, the more susceptible the arch is to buckle and loss of stability due to the increased eccentricity of compression load between the ends of the specimen. Due to radius alone, arch profiles losses about 18% of its cross-sectional resistance against compression.

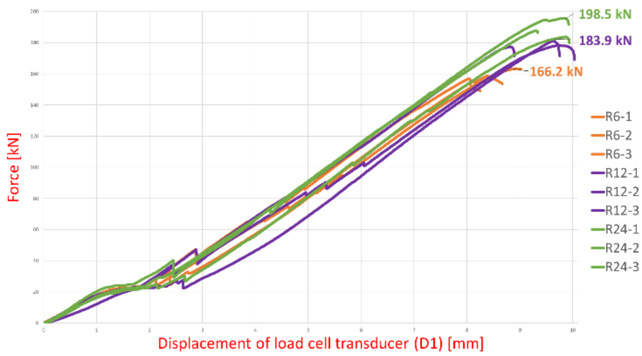

Figure 9 Force vs displacement curves for all 1.5mm thick arch profiles

Table 1 shows the ultimate strength and the corresponding displacements for all the specimens. Steel arch profiles with thickness of 1.5 mm has 55% higher ultimate load value than the 1.1 mm thick arch profiles due to a larger effective area to resist axial compressive forces.

Table 1 Compression tests results

Thickness (mm)	Radius (m)	Test	Ultimate force [kN]	Displacement corresponding Fu [mm]	Average Ultimate force [kN]	Standard Deviation
		Test 1	109.7	6.5		
	6	Test 2	102.1	6.0	**104.8**	**3.4**
		Test 3	102.6	6.1		
		Test 1	109.0	6.5		
1.1	12	Test 2	103.2	6.6	**108.7**	**4.4**
		Test 3	114.0	6.5		
		Test 1	122.2	8.2		
	24	Test 2	126.3	7.3	**123.6**	**1.9**
		Test 3	122.4	6.8		
		Test 1	99.3	6.9		
	6	Test 2	95.6	7.4	**97.3**	**1.6**
		Test 3	97.0	6.7		
		Test 1	118.3	7.1		
1.2	12	Test 2	117.4	7.9	**117.3**	**0.8**
		Test 3	116.4	7.1		
		Test 1	133.8	8.1		
	24	Test 2	133.0	7.5	**134.8**	**2.0**
		Test 3	137.6	7.8		
		Test 1	166.2	8.9		
	6	Test 2	159.6	8.0	**162.4**	**2.8**
		Test 3	161.4	8.4		
		Test 1	183.9	9.6		
1.5	12	Test 2	181.1	9.7	**181.7**	**1.6**
		Test 3	180.2	8.8		
		Test 1	198.5	9.8		
	24	Test 2	186.5	9.9	**191.8**	**5.0**
		Test 3	190.4	9.3		

The results indicate that the larger the curvature radius is, the stronger the member cross sectional resistance to compression forces is.

4.2 Stiffness tests results

The data recorded from the load cell and displacement sensors in horizontal stiffness tests were used to produce the load-displacement curves. The effect of steel plate thickness on horizontal stiffness of steel arches with a radius of 24 m are demonstrated using thicknesses of 1.1, 1.2 and 1.5 mm in Figure 10. Due to the slight nonlinearity observed when the maximum displacements reach 20 mm, the secant stiffness at ±15 mm in ascending linear phase was used to obtain the horizontal stiffness. The test results indicated that the 1.5 mm thick specimens have a higher spring value than steel arches with thicknesses of 1.1- and 1.2-mm. For all the thickness groups the increase of radius decreases stiffness as shown in Table 2.

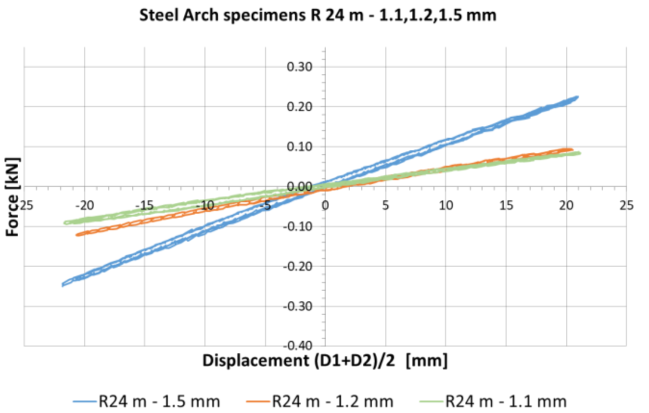

Figure 10 *Horizontal* Stiffness test results - Radius 24 m and I.1,1.2 & 1.5 mm thick specimens

Additionally, almost all the horizontal spring constants were lower than the vertical ones as indicated in Table 2. According to the tests, larger thickness of sample increased horizontal and vertical spring constants but increase of radius decreased the spring constants.

Table 2 Horizontal and Vertical Stiffness tests results

Test name	Curvature [m]	Horizontal Spring stiffness , K [N/mm²]	Vertical Spring stiffness, K [N/mm²]
t=1,1 mm			
R6 t 1,1 Test 1	R6	0.016	0.016
R6 t 1,1 Test 2		0.013	0.014
R12 t 1,1 Test 1	R12	0.009	0.010
R12 t 1,1 Test 2		0.007	0.011
R24 t 1,1 Test 1	R24	0.007	0.008
R24 t 1,1 Test 2		0.006	0.007
t=1,2 mm			
R6 t 1,1 Test 1	R6	0.020	0.025
R6 t 1,1 Test 2		0.020	0.025
R12 t 1,1 Test 1	R12	0.017	0.017
R12 t 1,1 Test 2		0.015	0.018
R24 t 1,1 Test 1	R24	0.009	0.010
R24 t 1,1 Test 2		0.012	0.010
t=1,5 mm			
R6 t 1,1 Test 1	R6	0.038	0.048
R6 t 1,1 Test 2		0.035	0.047
R12 t 1,1 Test 1	R12	0.017	0.032
R12 t 1,1 Test 2		0.017	0.031
R24 t 1,1 Test 1	R24	0.016	0.023
R24 t 1,1 Test 2		0.018	0.021

4.3 Theoretical effective area of cross section

The theoretical effective cross-section depends on the spring stiffness. Based on table 4.1 and 4.2 in SFS EN 1993-1-5, the effective widths b_{eff} were calculated for all the parts of the cross section. Before the calculation, the range of the dimensions were checked first. Table 3 lists down the measured geometrical dimensions of the idealized cross section. The maximum width-to-thickness ratio stated in table 5 in SFS-EN 1993-1-3 was applied to the preliminary check of the theoretical cross section. All checks passed except those of the plates e_1 and d_1 because they were not considered in SFS-EN 1993-1-3.

Table 3 Basic dimensions of the cross section

Basic dimensions	Notation	Value
Lower flange width	b	205 mm
Web length	S_{w1} and S_{w2}	216 mm
Web height	h_{w1} and h_{w2}	176 mm
Upper flange 1 width	b_1	70 mm
Upper flange 2 width	b_2	90 mm
Triple edge fold internal 1 width	c_1	26 mm
Triple edge fold internal 2 +-width	d_1	32 mm
Triple edge fold outstand width	e_1	16 mm
Double edge fold internal width	c_2	30 mm
Double edge fold outstand width	d_2	20 mm
Element height	h_1 and h_2	205 mm
Element width	b_{total}	649 mm

The flat cross section under the compression uniaxial load was determined by following the design code SFS EN 1993-1-3. Additionally, the *K* values based on tests with a radius of 24 m were used to calculate the effective thickness of the edge stiffeners.

Table 4 Theoretical Effective area of cross sections

Arch thickness [mm]	Effective Area [mm^2]
1.1	**258.4**
1.2	**307.5**
1.5	**468.8**

The resistance of the flat section can be calculated by multiplying the effective cross section with the material strength. The calculation of the axial resistance is based on the centroid of the effective cross-section.

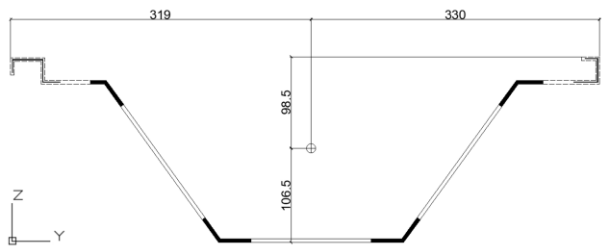

Figure 11 Theoretical calculation of centroids of cross-section

The centroid of the flat effective cross section was found to be about 98.5 mm in z-direction and 330 mm in y-direction from the double edge stiffener as show in figure 11.

4.4 Material properties

To determine the cross-sectional resistance using the effective cross-section, the coupon tests were also performed. The coupons were cut off from the flat area of the upper flanges of the arch specimens. The steel grade of the specimens was S350GD. However, the cold forming enhanced the yield strength of the material. The elastic modulus, yield strength and ultimate strength measured are shown in table 5. The results show that the 1.1 mm, 1.2 mm, and 1.5 mm thick samples had an average yield strength of 381 MPa, 389 MPa, 360 MPa, and average ultimate tensile strength of 457 MPa, 454 MPa and 437 MPa, respectively. Additionally, the relative capacity for strain hardening after yielding was 20 %, 17% and 21 % for 1.1 mm, 1.2 mm, and 1.5 mm thick samples, respectively.

Table 5 Material test results for R24 steel arch specimens

Type	Thickness mm	Width mm	Elastic modulus GPa	Lower yield limit MPa	Higher yield limit MPa	Ultimate strength Mpa	Elongation %	Yield strength Average MPa	Ultimate strength Average MPa
1.1mm R24 Test 1	1.10	20.3	190.6	384.4	387.3	458.7	2.4	**380.7**	**457.6**
1.1mm R24 Test 2	1.10	20.1	198.7	379.8	394.5	458.4	2.3		
1.1mm R24 Test 3	1.10	20.7	196.3	379.2	387.8	456.9	2.0		
1.1mm R24 Test 4	1.10	20.5	187.4	379.3	388.0	456.2	2.4		
1.2mm R24 Test 1	1.22	20.4	187.8	409.0	429.5	471.0	4.0	**388.8**	**454.2**
1.2mm R24 Test 2	1.21	20.4	188.2	406.2	436.5	474.1	3.6		
1.2mm R24 Test 3	1.22	19.6	201.0	369.9	394.4	436.4	3.1		
1.2mm R24 Test 4	1.22	20.2	209.9	370.0	393.2	435.4	3.0		
1.5mm R24 Test 1	1.52	20.2	197.0	358.9	365.2	437.9	1.4	**360.2**	**437.4**
1,5mm R24 Test 2	1.52	20.4	188.8	358.2	364.2	434.8	1.7		
1,5mm R24 Test 3	1.51	20.1	181.5	356.8	364.1	435.5	1.7		
1,5mm R24 Test 4	1.52	20.7	211.7	366.8	371.6	441.2	1.7		

4.5 Analysis of test and theoretical results

The cross-sectional resistance of the steel arches with corrugations under compression load is determined according to the results shown in table 6. It is recommended to correct the theoretically calculated effective cross section by the correction factors considering both the corrugations and strength enhancement due to cold forming. The correction factor is calculated as the ratio of theoretical values with respect to test values. Table 6 shows that the correction factors are varied between 0.90 to 1.37 as the thickness and radius of the steel arch change.

Table 6 Correction factors based on theoretical and tests results

Thickness $[mm]$	Radius of Arch $[m]$	Tested (A_{eff}) $[mm^2]$	Theoretical (A_{eff}) $[mm^2]$	Geometry enhancement factor (**β1**) $\frac{A_{eff.test}}{A_{eff.theory}}$	Correction factor (**β2**) $\frac{f_{y.test}}{f_{y.theory}}$	Corrugation correction factor **(β) = (β1)*(β2)**
1.1	6	275.8	258.4	1.07	1.09	**1.16**
	12	286.1		1.11		**1.20**
	24	325.3		1.26		**1.37**
1.2	6	250.3	307.5	0.81	1.11	**0.90**
	12	301.7		0.98		**1.09**
	24	346.7		1.13		**1.25**
1.5	6	451.1	468.8	0.96	1.03	**0.99**
	12	504.7		1.08		**1.11**
	24	532.8		1.14		**1.17**

5 Conclusion

This paper presents an analytical approach to determine the effective properties of corrugated steel arch profiles under uniaxial compression load based on the results of experimental tests. The compression test results show that the steel arch profiles with a thickness of 1.5 mm has 55% higher ultimate load value than the arch profiles with a thickness of 1.1 mm due to a larger effective area to resist axial compressive forces. The results also indicate that a larger radius of arch increases the ultimate load carrying capacity. The smaller the arch radius, the more susceptible it is to fail due to increased eccentricity of compression load along the arch span. Due to radius alone, arch profiles losses about 18% of their cross-sectional resistance to compression. The horizontal and vertical spring stiffness tests revealed that a larger plate thickness increases the stiffness whereas a larger radius of steel arches decreases it.

The method for determining the corrugation correction factor (β) was explained in this paper step by step. The highest correction factors of the arch profiles received were 1.37, 1.25 and 1.17 for plate thicknesses of 1.1 mm, 1.2 mm, and 1.5 mm, respectively.

Acknowledgement

The research was carried out in collaboration with a Finnish construction company. Tests are carried out in HAMK Tech research centre. The authors would like to acknowledge the supports of laboratory personnel.

6 References

[1] American Society of Civil Engineers. (1998) *Minimum design load for buildings and other structures*. New York.

[2] NASA. (2000) *Hurricane worthy. Spaceport News 39(19), National Aeronautics and Space Administration*. Florida: Kennedy Space Centre.

[3] European Committee for Standardisation. (2006) *EN 1993-1-3: Eurocode 3: Design of Steel Structures - Part 1-3: General Rules - Supplementary Rules for Cold-Formed Members and Sheeting*.

[4] European Committee for Standardisation. (2006) *EN 1993-1-5: Eurocode 3: Design of Steel Structures - Part 1-5, General rules - Plated structural elements*.

[5] Artur Piekarczuk (2019). *Experimental and numerical studies of double corrugated steel arch panels*. Thin-Walled Structures 140, p.60-73

[6] Piekarczuk, A., Więch, P., Kuczyński, K., & Walentynski, R.A. (2021). *Experimental and computational approaches to the evaluation of double corrugated arch structures*. A review of the latest advancements. Archives of Civil Engineering 67, p.7-35.

[7] D. Zhdanov, V. Ulasevich. (2016*) A nonlinear analysis method for arch-shaped shell roofs made of cold-formed steel profiles*. Civil and Environmental Engineering 4, p.187-191

[8] Piekarczuk, A., Więch, P., & Cybulski, R.J. (2019). *Experimental method to evaluate the load-carrying capacity of double corrugated sheet profiles*. Thin-Walled Structures 144